

PARALLEL IMAGING FOR MOTION CORRECTION IN NEONATAL BRAIN MR RECONSTRUCTION

Lucilio Cordero-Grande^{1,2}, Emer Hughes^{1,2}, Rui Pedro A. G. Teixeira^{1,2}, and Joseph V. Hajnal^{1,2}

¹Centre for the Developing Brain, King's College London, London, London, United Kingdom, ²Division of Imaging Sciences and Biomedical Engineering, King's College London, London, London, United Kingdom

Target audience. Motion can occur within the duration of a MR scan largely affecting the imaging quality. In multi-shot or segmented acquisitions, a fraction of the k -space is acquired within a RF excitation with less blurred and noisy images than in single-shot acquisitions. However, motion is likely to occur among different shots, as they are acquired distant in time ¹. This is the case, for instance, of newborn imaging, where usually the subjects move in the scanner.

Purpose. The paper is focused on retrospective rigid motion correction for brain neonatal imaging. We restrict to within-plane motion to obtain the best possible quality slices as a first step for a 3D interslice alignment technique such as ². The method is devised to overcome the limitations of related contributions ^{3,4,5}, namely, (1) parallel imaging is used so that the joint motion correction and image reconstruction becomes overconstrained and consequently less prior information is needed, (2) no assumptions about motion magnitude are performed, and (3) rigid transforms are formulated in such a way that no blurring is introduced in the presence of motion as no regridding is applied.

Methods. Joint motion correction and reconstruction may be formulated in matrix form as $(\mathbf{x}, \mathbf{T}) = \arg\min_{\mathbf{x}, \mathbf{T}} \|\mathbf{M}\mathbf{F}_2\mathbf{S}\mathbf{T}\mathbf{x} - \mathbf{y}\|_2^2$, where \mathbf{y} denotes the measured data, \mathbf{x} the image to be reconstructed, \mathbf{T} the transform matrix, \mathbf{S} the sensitivity matrix, \mathbf{F}_2 the Fourier transform in the phase encoding (PE) direction and \mathbf{M} a sampling mask. The forward model for this formulation is depicted in Fig. 1. The rigid transform \mathbf{T} is modeled on the basis of ⁶ to perform high quality rotations without regridding by decomposing the rotational component of motion into three consecutive shears. To make it computationally tractable, the joint problem is addressed in an alternating fashion by iteratively solving for $\mathbf{x} = \arg\min_{\mathbf{x}} \|\mathbf{M}\mathbf{F}_2\mathbf{S}\mathbf{T}\mathbf{x} - \mathbf{y}\|_2^2$ and $\mathbf{T} = \arg\min_{\mathbf{T}} \|\mathbf{M}\mathbf{F}_2\mathbf{S}\mathbf{T}\mathbf{x} - \mathbf{y}\|_2^2$. The first subproblem has been considered in ⁷, where the conjugate gradient allows to obtain a solution. As for the second, the reason it is solvable is that the coil array may be used to estimate the position of the object inside the scanner, i.e., the image reconstruction problem is overdetermined. The solution must satisfy $\partial \|\mathbf{M}\mathbf{F}_2\mathbf{S}\mathbf{T}\mathbf{x} - \mathbf{y}\|_2^2 / \partial \mathbf{q}_{in} = 0$, with n indexing the shots (which correspond to different motion states) and \mathbf{q}_{in} the transform parameters. We have resorted to the Newton method for solving this system of equations. A multiresolution scheme is employed to accelerate computations and help in avoiding local optima of the joint problem. Additionally, the model is extended by introducing a LORAKS prior ⁸ on the reconstructed images, which, by promoting limited spatial support and slowly varying phase, also helps the method to escape from local optima.

Results. We have applied the procedure to a synthetically motion corrupted adult volunteer T_2 brain image where 12 shots are used to sample 192 PE lines (see Fig. 2). In addition, it has been applied to the reconstruction of neonatal brain images acquired by a 3T Philips Achieva TX using: (1) A TSE T_2 sequence with acquired voxel size $1 \times 1 \times 2 \text{ mm}$ (with a slice gap of -1 mm to help 3D reconstructions in the presence of motion ²), $T_E = 156 \text{ ms}$, $T_R = 10 \text{ s}$, $\alpha = 90^\circ$, and a dedicated 32-channel head coil array. Axial and sagittal views are acquired, in the first case with 96 PE lines, $N = 8$ shots and a SENSE factor of 1.25, and in the second with 120 lines, $N = 10$, and SENSE 1.2. (2) A TIR T_1 sequence with same resolution and coil array, $T_E = 8 \text{ ms}$, $T_R = 4.795 \text{ s}$, $\alpha = 90^\circ$, acquired in the axial view, with 112 lines, $N = 16$, and SENSE 1.07. A number of 16 axial T_2 , 16 sagittal T_2 and 5 T_1 volumes have been reconstructed with the proposed method. Assessment of the reconstruction quality is provided in Table 1 whereas in Fig. 3 a visual example is provided for each of the aforementioned sequences.

Discussion. Results on synthetic data in Fig. 2, with complete motion recovery, show the potential of the proposed approach even in cases in which large motion artifacts are present in the image and a relatively large number of shots is used. Results on real data have shown a significant enhancement in the quality of reconstructed images (see Table 1). The arrows in Fig. 3 point to some locations where this enhancement is most clearly noticeable. In the axial T_2 case the motion-corrected reconstruction has turned a useless image into one in which brain structures are clearly identifiable. Most striking benefits of the proposed technique are elimination or decrease of confounding artifacts, contrast improvement, better resolved structures and emergence of new anatomical details. Additionally, no adverse side effects have been observed when applying the joint reconstruction versus reconstruction without motion estimation.

Conclusion. We have reported a flexible and powerful framework for the reconstruction of multi-shot images in the presence of motion which has significantly enhanced the quality of neonatal brain images. The motion of the subject in the scanner is inferred using the information provided by the array of coils and no resolution is lost due to the sinc-based interpolation used for rigid transforms. The method provides good results under the within-plane rigid motion assumption so we are currently working in its 3D and elastic extensions.

References. 1. Bernstein, M.A., King, K.F., Zhou, X.J., *Handbook of MRI Pulse Sequences*, Elsevier Academic Press; 2004. 2. Kuklisova-Murgasova, M., Quaghebeur, G., et al., *Med. Image Anal.*, 16:1550-64; 2012. 3. Loktyushin, A., Nickisch, H., et al., *Magn. Reson. Med.*, 70:1608-18; 2013. 4. Loktyushin, A., Nickisch, H., et al., *Magn. Reson. Med.*, in press, DOI: 10.1002/mrm.25266; 2014. 5. Odille, F., Vuissoz, P.-A., et al., *Magn. Reson. Med.*, 60:146-57; 2008. 6. Unser, M., Thévenaz, P., Yaroslavsky, L., *IEEE Trans. Image Process.*, 4(10):1375-81; 1995. 7. Batchelor, P.G., Atkinson, D., et al., *Magn. Reson. Med.*, 54:1273-80; 2005. 8. Haldar, J.P., *IEEE Trans. Med. Imaging*, 33(3):668-681; 2014.

Acknowledgements. The authors acknowledge financial support the Department of Health via the National Institute for Health Research (NIHR) comprehensive Biomedical Research Centre award to Guy's & St Thomas' NHS Foundation Trust in partnership with King's College London (KCL) and King's College Hospital NHS Foundation Trust. The research leading to these results has received funding from the European Research Council under the European Union's Seventh Framework Programme (FP/2007-2013) / ERC Grant Agreement n. 319456. This work was also supported by Medical Research Council (MRC) strategic grant MR/K006355/1. The authors also acknowledge the Department of Perinatal Imaging & Health at KCL.

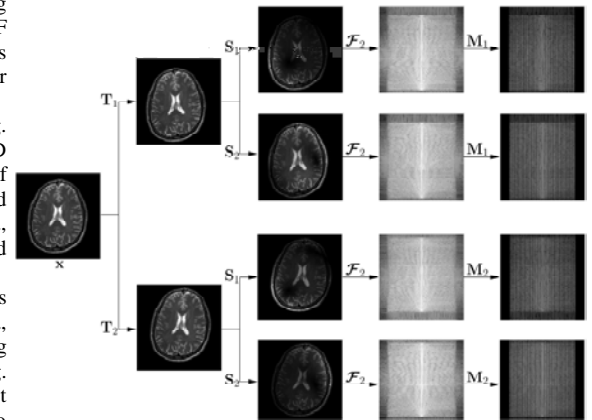


Fig. 1: Forward model of the multi-shot measurement process in the presence of motion.

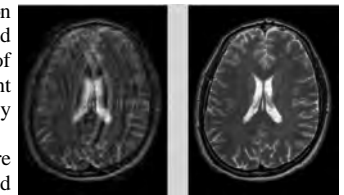


Fig. 2: Motion corrected reconstruction in simulated data. Left: corrupted. Right: corrected.

	Axial T_2	Sagittal T_2	Axial T_1
No motion	7	2	2
Corrupted	9	14	3
Small improvement	8	9	1
Large improvement	1	5	2

Table 1: Performance of motion corrected reconstruction in real data.

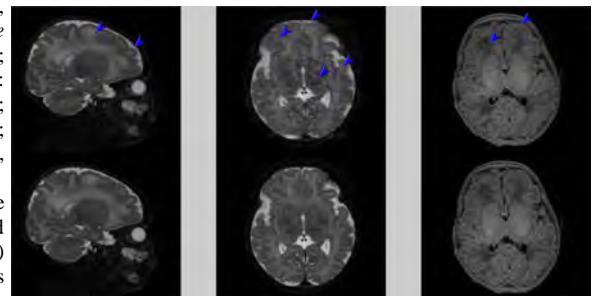


Fig. 3: Motion corrected reconstruction in real data. Top: reconstruction without motion correction. Bottom: reconstruction with motion correction. Left: Sagittal T_2 . Center: Axial T_2 . Right: Axial T_1 .